Electronic Supplementary Information for

A dual cross-linked aromatic polythiourea gate dielectric with multifunctional capabilities for organic field-effect transistors

Sungmi Yoo,‡[a] Hyunjin Park,‡[a] Yong Seok Kim,[ab] Jong Chan Won,[ab] Dong-Gyun Kim,*[a] and Yun Ho Kim*[ab]

[a]Advanced Materials Division, Korea Research Institute of Chemical Technology, 141 Gajeong-ro, Yuseong-gu, Daejeon 34114, Republic of Korea

[b]Chemical Convergence Materials and Processes, University of Science and Technology, 217 Gajeong-ro, Yuseong-gu, Daejeon 34114, Republic of Korea

‡These authors contributed equally to this work.

*Corresponding author: D.-G. Kim (E–mail: dgkim@krict.re.kr)
Y. H. Kim (E–mail: yunho@krict.re.kr)

Table of Contents

Experimental Section

Materials

1,1'-Thiocarbonyldiimidazole (TCDI, tech. 90%, Alfa Aesar), dinaphtho[2,3-b:2',3'-f]thieno[3,2-b]thiophene (DNTT, >99%, Sigma-Aldrich), aluminum(III) nitrate nonahydrate ($Al(NO_3)_3 \cdot 9H_2O$, >99.997%, Sigma-Aldrich), octadecylphosphonic acid (ODPA, 97%, Sigma-Aldrich), pentaerythritol tetrakis(3-mercaptopropionate) (PETMP, >95%, Sigma-Aldrich), N-methyl-2-pyrrolidone (NMP, anhydrous, 99.5%, Sigma-Aldrich), 4,4'-Oxydianiline (ODA, >98%, Tokyo Chemical Industry) were used as received. All other reagents and solvents were used as received from standard vendors.

Synthesis of Polythiourea from TCDI and ODA

Aromatic polythiourea (PTU) was synthesized by polycondensation of TCDI and ODA in NMP (Fig. S1). Preparation procedure was conducted under a nitrogen atmosphere in a glove box (<0.1 ppm of H_2O and O_2). ODA (5.1 g, 25 mmol) and NMP (60 mL) were placed into a 100 mL round-bottomed flask with a magnetic stirring bar, and TCDI (5.0 g, 28 mmol) was added into the flask under stirring. The reaction flask sealed with stopper was transferred to a thermostatted oil bath at 90 °C outside the glove box. After stirred for 24 h, the solution was precipitated into an excess of methanol. The dissolution-precipitation procedure was repeated three times. The resulting precipitate was subsequently dried under vacuum at 70 °C for 24 h, yielding a yellowish white solid (5.2 g, 72%). ^{1}H NMR (400 MHz, DMSO-d_6, δ/ppm, tetramethylsilane (TMS) ref) (Fig. S2): 9.70 (br, C(S)N*H*), 9.60 (br, C(S)N*H* of end-group), 7.45–7.43, 6.99–6.97 (Ar-*H*), 7.33–7.31, 6.83–6.80, 6.77–6.75, 6.59–6.57 (Ar-*H* of end-group). GPC-RI analysis: number-average molecular weight (M_n) = 12,700 g mol^{-1}, molecular weight dispersity ($Đ$) = 1.92.

Fabrication of Cross-Linked PTU Thin Film

Dual cross-linked PTU films are designated as c-PTU#, where # indicates the molar feed ratio of the thiol group of PETMP to the thiourea group of PTU ([thiol]/[thiourea]) in the film. The # was controlled from 0.2 to 1.0 at 0.2 intervals to optimize the dielectric properties of c-PTUs. To prepare 200 nm-thick c-PTU films, appropriate amounts of PTU, PETMP, and Irgacure® 819 (a photo-initiator, 5 wt% to the PTU and PETMP) were dissolved in NMP. The total feed concentration was 9 wt% in NMP. The homogeneous mixture solution was spin-coated on a glass substrate and thermally annealed at 90 °C for 1 min. Then, ultraviolet (UV, λ = 365 nm, 4 J cm^{-2}) was irradiated at room temperature to induce the cross-linking reaction between PTU and PETMP. The resultant thin film was thermally annealed at 90 °C for 30 min, followed by vacuum drying at room temperature overnight. For comparison purposes, PTU thin film with similar thickness was also prepared without the PETMP and photo-initiator. Photo-patterned c-PTU thin film was fabricated using the similar procedure, but the UV exposure of 4 J cm^{-2} was performed on the spin-coated thin film through 25 μm-line-patterned shadow mask (Fig. S11). After thermal treatment at 90 °C for 30 min, the c-PTU thin film was immersed in NMP solvent for 20 s to develop the patterns and dried under N_2 flow.

Metal-Oxide-Assisted Surface Treatment for c-PTU0.6 Thin Film

Metal-oxide-assisted surface treatment (MAST) method[S1] was applied to modify the surface property of c-PTU0.6 thin film. Solution-processed MAST method was composed of α-Al_2O_3 layer fabrication and self-assembled monolayer (SAM) treatment (Fig. S12). To fabricate 20 nm-thick α-Al_2O_3 layer, 7 wt% solution of aluminum(III) nitrate nonahydrate in 2-butoxyethanol was deposited on the c-PTU0.6 thin film by spin-coating at 2000 rpm for 30 s, followed by thermal treatment on a hot plate at 90 °C for 10 min and 200 °C for 40 min. For the additional SAM treatment, 0.01 wt% solution of ODPA in ethanol was spin-coated on the α -Al_2O_3/c-PTU0.6 double layer thin film at 3000 rpm for 30 s, followed by thermal treatment at 150 °C for 3 min. The excess ODPA residues were washed several times with ethanol. Thickness of ODPA layer was about 2 nm. [S2]

Device Fabrication

For the fabrication of gate dielectric film, a substrate (glass) was cleaned by sonication in deionized (DI) water, acetone, and isopropanol sequentially for every 20 min at room

temperature. Then, the cleaned substrate was dried in a convection oven at 60 °C for 30 min before use. Metal-insulator-metal (MIM) capacitor with the active area of 1 mm^2 was fabricated by depositing the PTU and c-PTU thin films via the above thin-film fabrication procedure between thermally deposited top and bottom aluminum (Al) electrodes. For fabrication of bottom-gate, top-contact organic field-effect transistors (OFETs), a 30 nm-thick Al gate electrode was deposited on the substrate. Once the PTU-based gate dielectrics were deposited, 50 nm-thick DNTT was thermally evaporated on the gate dielectric layers. Finally, a 50 nm-thick gold (Au) was thermally evaporated on the DNTT layers through shadow mask for the formation of source/drain electrodes with a channel length (L) and width (W) of 100 μm and 1500 μm, respectively. The thermal evaporation rate was 0.3 Å sec^{-1} for the Al, DNTT, and Au, respectively, at a pressure of below 3×10^{-6} torr.

Instrumentation and Characterization

^{1}H NMR spectrum was recorded on a Bruker Ascend 400 MHz using DMSO-d_6 as a solvent. Number-average molecular weight (M_n) and molecular weight dispersity of PTU were determined by gel permeation chromatography (GPC) in dimethyl acetamide (DMAc, with 0.05 M LiBr), using a Waters 1515 Isocratic HPLC pump, a Shodex KF-805L column, and a Waters 2414 Refractive index (RI) detector at 40 °C. The GPC-RI elution time data were calibrated with narrow-distribution polystyrene standards. Thermogravimetric analysis (TGA) was performed using TA Instruments Q5000 under a nitrogene atmosphere. Differential scanning calorimetry (DSC) was run using a TA Instruments DSC Q1000 under a nitrogen atmosphere. Fourier-transform infrared (FTIR) spectra were recorded on a Bruker VERTEX 80v FTIR spectrometer. Raman spectra were collected using Bruker FRA 106/S spectrometer with a 1064 nm Nd:YAG laser. Wide angle X-ray scattering (WAXS) profiles obtained using Rigaku Ultima IV with Scintillation counter detector. The applied max power, voltage, and current were 2kW, 40kV, and 40mA, respectively. The thin-film thickness was measured with an alpha-step surface profiler (α-step DC50, KLA-Tencor). The contact angles of DI water and diiodomethane were measured using PHOENIX450 contact angle analyzer. Atomic force microscopy (AFM) images were recorded with a tapping mode microscope (Nanoscope IV, Digital Instrument). The capacitance was measured with a precision LCR meter (E4980A, Agilent). The electrical characteristics of OFETs were measured with a semiconductor parameter analyzer (E5272, Agilent). All electrical measurements were performed under ambient atmosphere condition.

Synthesis of Aromatic Polythiourea

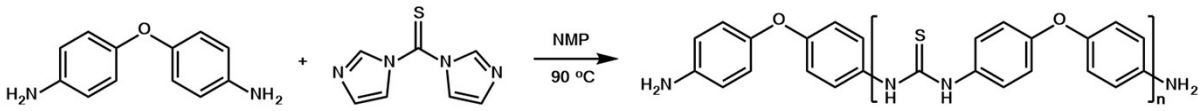

Fig. S1 Synthesis of aromatic PTU from TCDI and ODA in NMP.

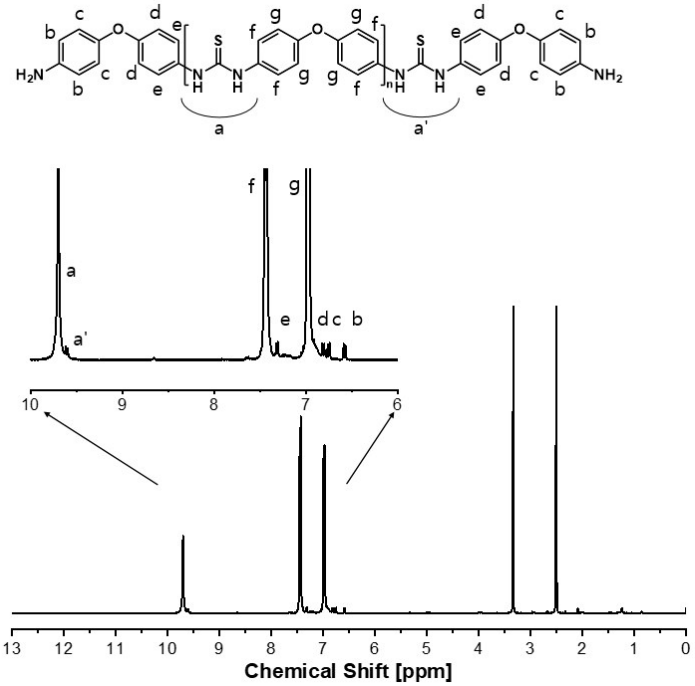

Fig. S2 ^{1}H NMR spectra of PTU.

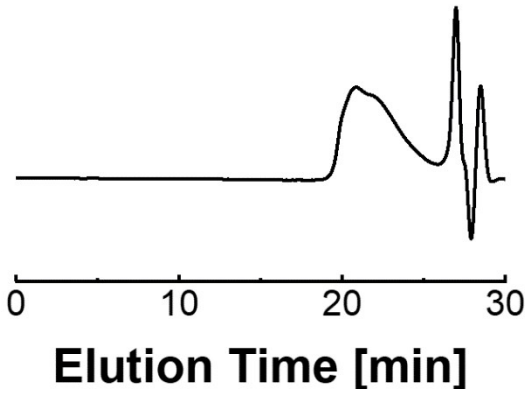

Fig. S3 GPC trace of PTU in DMAc.

Table S1 Composition of PTU and PETMP in the c-PTU#s.

Sample[a]	Molar feed ratio (#)
	[thiol] / [thiourea]
c-PTU0.2	0.2 / 1.0
c-PTU0.4	0.4 / 1.0
c-PTU0.6	0.6 / 1.0
c-PTU0.8	0.8 / 1.0
c-PTU1.0	1.0 / 1.0

[a] Irgacure® 819 (a photo-initiator, 5 wt% to the PTU and PETMP) was added. The total feed concentration was 9 wt% in NMP.

Structural and Thermal Characterization of Cross-Linked PTU (c-PTU) Thin Films

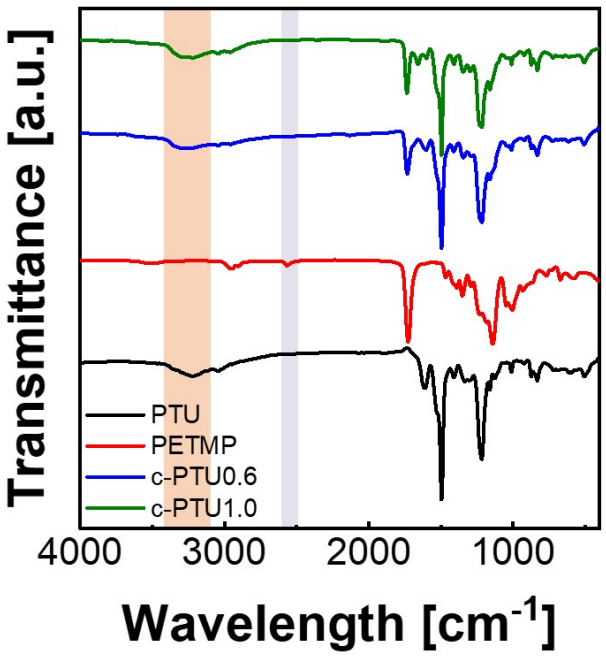

Fig. S4 FTIR spectra of PTU, PETMP, c-PTU0.6 and c-PTU1.0.

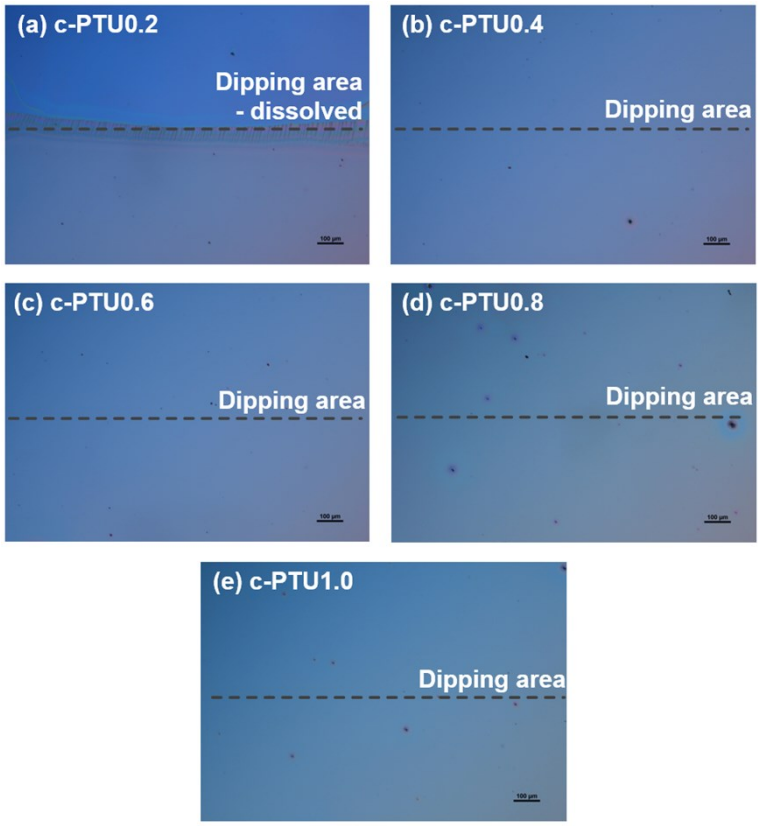

Fig. S5 OM images of c-PTU thin films after immersing in NMP solvent.

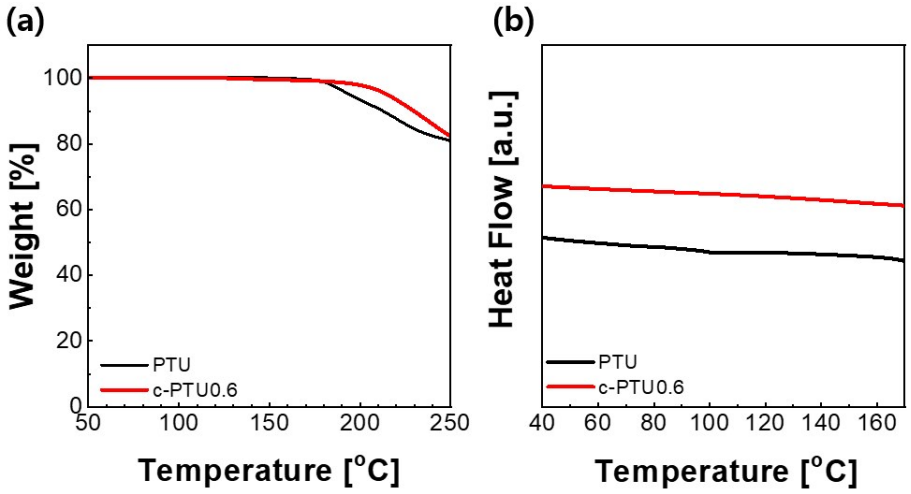

Fig. S6 (a) TGA and (b) DSC analysis of PTU and c-PTU0.6.

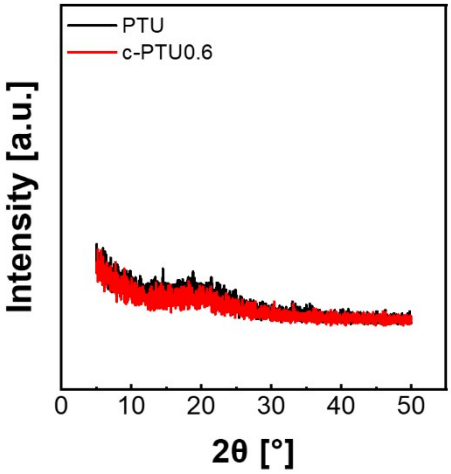

Fig. S7 WAXS profiles of PTU and c-PTU0.6.

Electrical Properties of c-PTU and Surface-Treated c-PTU (sc-PTU) Thin Films

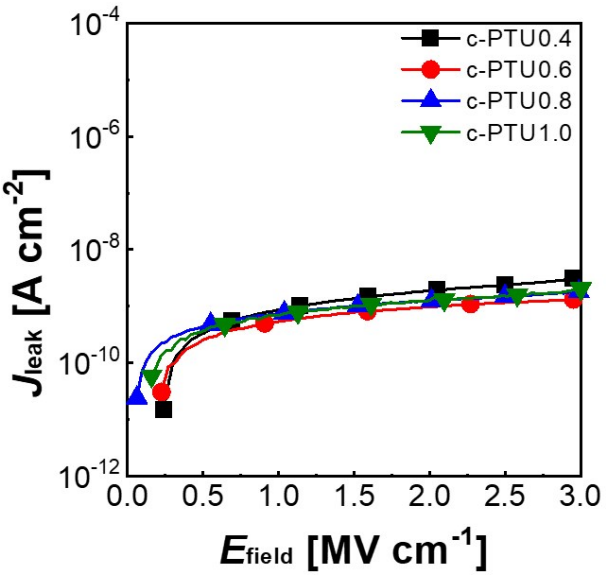

Fig. S8 Leakage current densities (J_{leak}) as function of electric field (E_{field}) of c-PTU thin films.

Table S2 Leakage current densities of c-PTU thin films.

	Thickness [nm]	Leakage Current Density[a] [A cm^{-2}]
c-PTU0.4	341	3.19×10^{-9}
c-PTU0.6	309	1.36×10^{-9}
c-PTU0.8	341	2.03×10^{-9}
c-PTU1.0	318	2.12×10^{-9}

[a] Measured at 3 MV cm^{-1}. [b] Measured at 1 kHz.

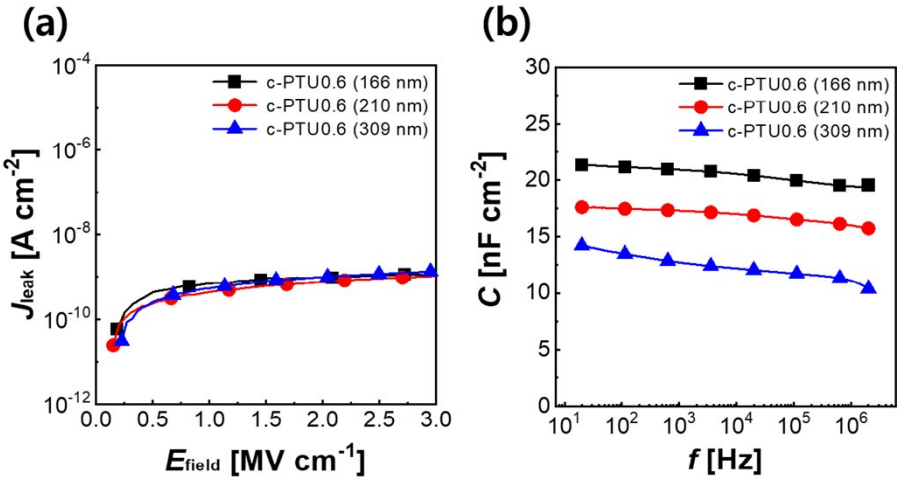

Fig. S9 (a) J_{leak} as function of E_{field} and (b) capacitances as function of frequency of c-PTU0.6 thin films with different thicknesses.

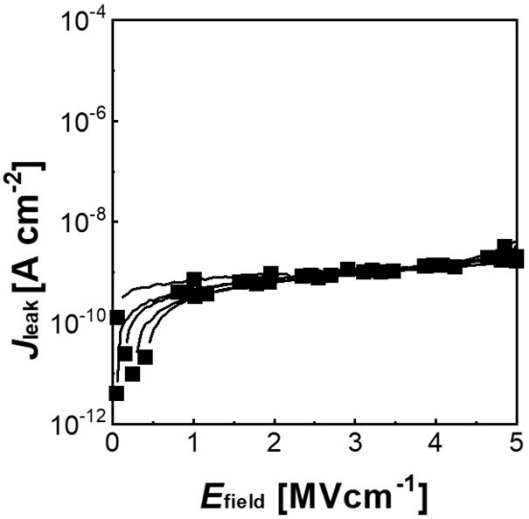

Fig. S10 Reproducibility of J_{leak} of 200 nm-thick c-PTU0.6 thin films from five different MIM capacitors.

Table S3 Comparison of breakdown electric field of polymer gate dielectrics in MIM capacitors.

	Ref.	Thickness [nm]	T^a [°C]	ε_r	Electric field [MV cm^{-1}]		E_{bd} [MV cm^{-1}]
					10^{-10} A/cm^2	10^{-8} A/cm^2	
PVP[b]	S3	12	200	3.2 (100 kHz)	-	1.0	> 3.0
	S4	103	150	4.3 (1 kHz)	-	0.5	-
	S5	200	130	4.5	-	1	< 5
	S6	200	180	5 (100 Hz)	-	0.1	> 1
	S7	60	200	2.5	-	-	< 1
	S8	250	180	5.5	-	-	< 0.5
	S9	350	180	5.66 (1 MHz)	-	-	< 0.5
PVA[c]	S10	537	100	6.0 (100 kHz)	1.0	-	> 1.9
	S11	248	100	6.3 (1 kHz)	-	2	> 2
	S12	300	100	3.2 (1 MHz)	-	0.2	0.45
PMMA[d]	S13	100	100	3.9(10 kHz)	-	1	-
	S14	100	120	3 (1 kHz)	-	1	< 4
Polyimide	S3	9	250	2.6 (100 kHz)	-	1.0	> 2.5
	S15	200	75	3.2 (100 Hz)	1	2	< 2.5
	S16	300	-	3.3 (10 kHz)	3	-	> 3
Parylene	S17	200	-	3.1	-	-	2.7
	S18	330	-	2.61 (1 MHz)	-	-	2.35
c-PTU0.6	This work	200	90	4.1 (1 kHz)	< 5	< 5	> 5

[a] Processing temperature, [b] Poly(4-vinylphenol), [c] Poly(vinyl alcohol), [d] Poly(methyl methacrylate)

Table S4 Comparison of dielectric constants for polymer gate dielectrics before and after cross-linking reaction.

	Ref.	T_C[a] [°C]	ε_r	
			Before	*After*
PVP[b]	S19	200	4.0 (10 Hz)	3.4
	S20	200	3.9 (1 MHz)	3.5
PVA[c]	S10	110	6.9 (100 kHz)	6.0
	S11	100	6.34 (1 kHz)	6.30
PMMA[d]	S12	200	3.15 (1 MHz)	2.8
c-PTU0.6	This work	90	3.9 (1 kHz)	4.1

[a] Crocessing temperature, [b] Poly(4-vinylphenol), [c] Poly(vinyl alcohol), [d] Poly(methyl methacrylate)

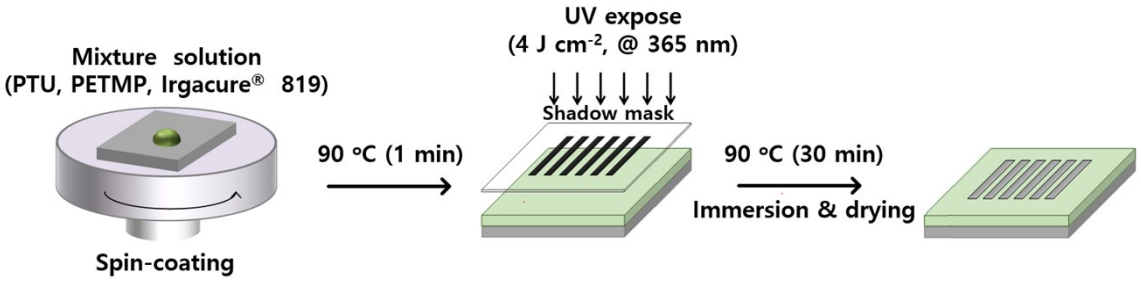

Fig. S11 Schematic illustration of the photo-patterning process for c-PTU thin film.

Surface Properties of c-PTU and sc-PTU Thin Films

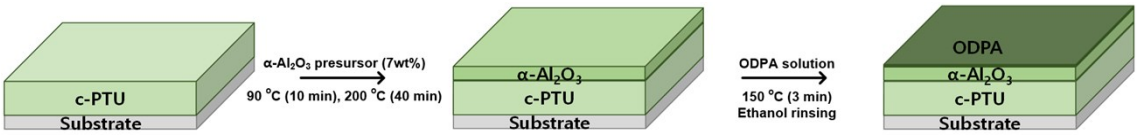

Fig. S12 Schematic illustration of MAST process for c-PTU thin film.

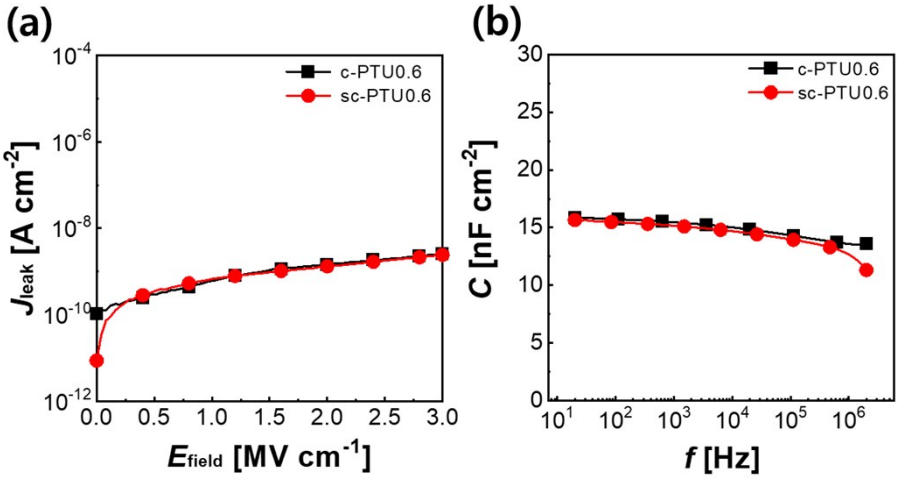

Fig. S13 (a) J_{leak} as function of E_{field} and (b) capacitance as function of frequency of c-PTU0.6 and sc-PTU0.6 thin films.

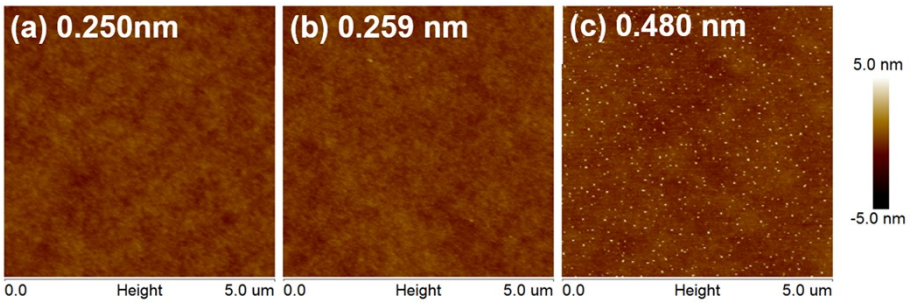

Fig. S14 (a, b) AFM images of c-PTU0.6 thin film surfaces (a) before and (b) after immersion in NMP. (c) AFM images of sc-PTU0.6 thin film surface.

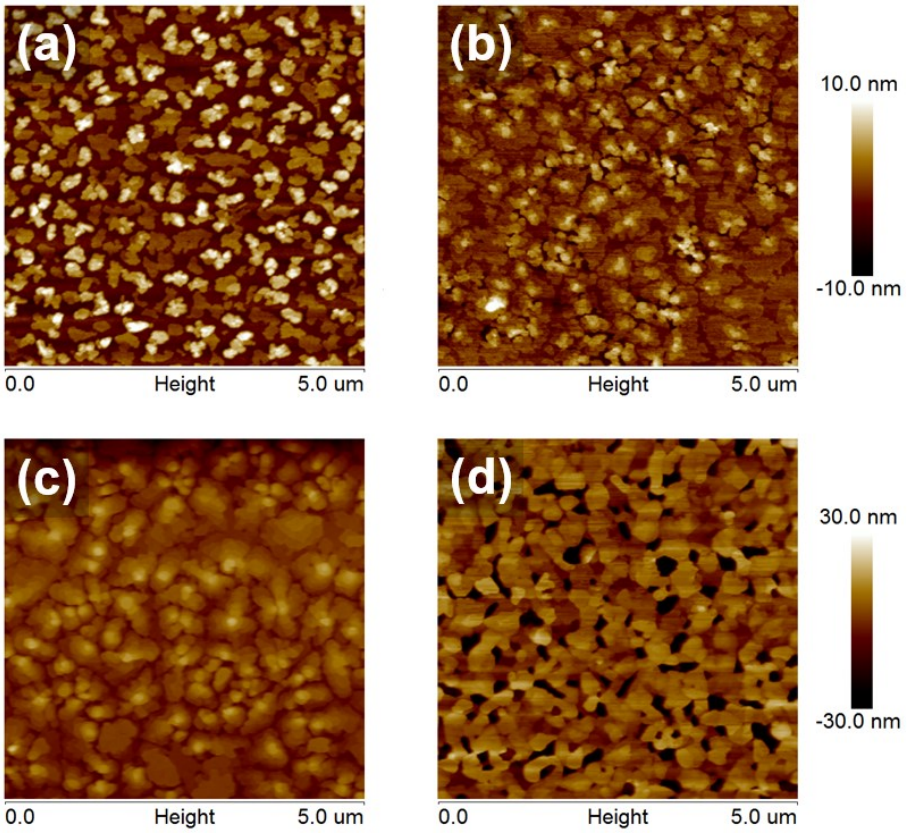

Fig. S15 (a-c) AFM images of (a) 5 nm, (b) 10 nm, and (c) 60 nm DNTT thin films deposited on c-PTU0.6 thin films. (d) AFM image of 60 nm DNTT thin film deposited on sc-PTU0.6 thin film.

Table S5 DI water and diiodomethane sessile drop contact angles and surface energies of the c-PTU0.6 and sc-PTU0.6 thin films.

	Water [°]	**Diiodomethane [°]**	**γ^p [polar, dyne cm^{-1}]**	**γ^d [dispersive, dyne cm^{-1}]**	**Surface Energy [γ, dyne cm^{-1}]**
c-PTU0.6	67.60	26.5	8.25	40.64	48.88
sc-PTU0.6	98.26	55.24	0.54	30.79	31.34

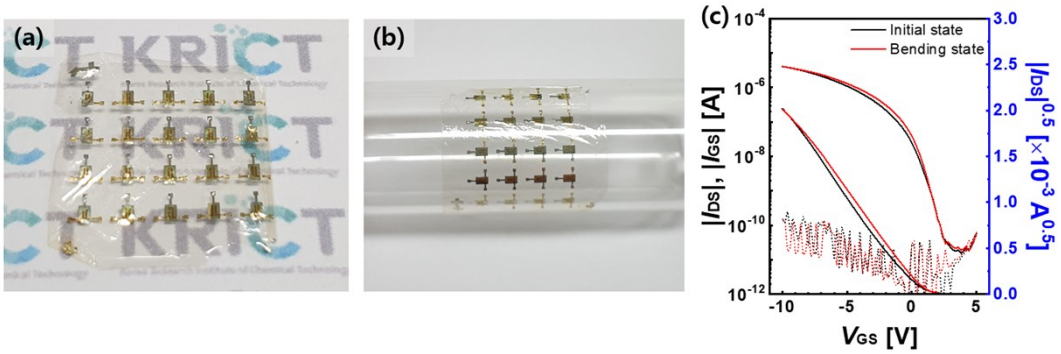

Fig. S16 Photographs of DNTT-based OFET integrated with 3 μm-thick poly-*para*-xylylene substrate as (a) fabricated and (b) bent. (c) Transfer curves for DNTT-based OFETs with sc-PTU gate dielectric as fabricated (black) and bent (red).

Table S6 Electrical characteristics of DNTT-based OFET integrated with poly-*para*-xylylene substrate as fabricated and bent.

Device state	μ **[cm²/Vs]**	V_{th} **[V]**	***SS*** **[V/decade]**	I_{on}/I_{off}
Initial state	0.251	-0.067	1.05	2.35×10^5
Bending state	0.203	0.77	0.82	1.81×10^5

References for Electronic Supplementary Information

S1 S. Kim, T. Ha, S. Yoo, J.-W. Ka, J. Kim, J. C. Won, D. H. Choi, K.-S. Jang and Y. H. Kim, *Phys. Chem. Chem. Phys.*, 2017, **19**, 15521–15529.

S2 H. Klauk, U. Zschieschang, J. Pflaum and M. Halik, *Nature*, 2007, **445**, 745–748.

S3 S. Y. Yang, S. H. Kim, K. Shin, H. Jeon and C. E. Park, *Appl. Phys. Lett.*, 2006, **88**, 2004–2007.

S4 L. Feng, C. Jiang, H. Ma, X. Guo and A. Nathan, *Org. Electron.*, 2016, **38**, 186–192.

S5 P. Vicca, S. Steudel, S. Smout, A. Raats, J. Genoe and P. Heremans, *Thin Solid Films*, 2010, **519**, 391–393.

S6 S. C., M. P. Joshi and V. Singh, *Microelectron. Eng.*, 2018, **198**, 85–92.

S7 K. Eum, K. Kim, J. Han and I. Chung, *J. Vac. Sci. Technol. A Vacuum, Surfaces, Film.*, 2010, **28**, 873–878.

S8 B. K. Tehrani, C. Mariotti, B. S. Cook, L. Roselli and M. M. Tentzeris, *Org. Electron.*, 2016, **29**, 135–141.

S9 K. Kim, N. Kwon and I. Chung, *Thin Solid Films*, 2014, **550**, 689–695.

S10 S. H. Jin, J. S. Yu, C. A. Lee, J. W. Kim, B. G. Park and J. D. Lee, *J. Korean Phys. Soc.*, 2004, **44**, 181–184.

S11 W. Sun, J. Zhao, S. Chen, X. Guo and Q. Zhang, *Synth. Met.*, 2019, **250**, 73–78.

S12 M. Na and S.-W. Rhee, *Org. Electron.*, 2006, **7**, 205–212.

S13 S. Jung, M. Albariqi, G. Gruntz, T. Al-Hathal, A. Peinado, E. Garcia-Caurel, Y. Nicolas, T. Toupance, Y. Bonnassieux and G. Horowitz, *ACS Appl. Mater. Interfaces*, 2016, **8**, 14701–14708.

S14 T. Tippo, C. Thanachayanont, P. Muthitamongkol, C. Junin, M. Hietschold and A. Thanachayanont, *Thin Solid Films*, 2013, **546**, 180–184.

S15 H. Park, S. Yoo, M. H. Yi, Y. H. Kim and S. Jung, *Org. Electron.*, 2019, **68**, 70–75.

S16 J. M. Won, H. J. Suk, D. Wee, Y. H. Kim, J. W. Ka, J. Kim, T. Ahn, M. H. Yi and K. S. Jang, *Org. Electron. physics, Mater. Appl.*, 2013, **14**, 1777–1786.

S17 K. Tsukagoshi, I. Yagi, K. Shigeto, K. Yanagisawa, J. Tanabe and Y. Aoyagi, *Appl. Phys. Lett.*, 2005, **87**, 183502.

S18 E. Y. Shin, E. Y. Choi and Y. Y. Noh, *Org. Electron.*, 2017, **46**, 14–21.

S19 H. Park, J. Kwon, B. Kang, W. Kim, Y.-H. Kim, K. Cho and S. Jung, *ACS Appl. Mater. Interfaces*, 2018, **10**, 24055–24063.

S20 D. K. Hwang, J. H. Park, J. Lee, J.-M. Choi, J. H. Kim, E. Kim and S. Im, *J. Electrochem. Soc.*, 2006, **153**, G23.